PLOS ONE

Retinal and cortical visual acuity in a common inbred albino mouse

Michelle Braha(iD), Vittorio Porciatti, Tsung-Han Chou(iD) *

Bascom Palmer Eye Institute, Miller School of Medicine, University of Miami, Miami, Florida, United States of America

* tchou@med.miami.edu

Abstract

While albino mice are widely used in research which includes the use of visually guided behavioral tests, information on their visual capability is scarce. We compared the spatial resolution (acuity) of albino mice (BALB/c) with that of pigmented mice (C57BL/6J). We used a high-throughput pattern electroretinogram (PERG) and pattern visual evoked potential (PVEP) method for objective assessment of retinal and cortical acuity, as well as optomotor head-tracking response/ reflex (OMR). We found that PERG, PVEP, and OMR acuities of C57BL/6J mice were all in the range of 0.5–0.6 cycles/degree (cyc/deg). BALB/c mice had PERG and PVEP acuities in the range of 0.1–0.2 cyc/deg but were unresponsive to OMR stimulus. Results indicate that retinal and cortical acuity can be reliably determined with electrophysiological methods in BALB/c mice, although PERG/PVEP acuities are lower than those of C57BL/6J mice. The reduced acuity of BALB/c mice appears to be primarily determined at retinal level.

Introduction

The study of visual capabilities in inbred mouse strains is of growing importance, as many behavioral tests used to characterize the effects of genetic manipulations rely on visual information [1]. BALB/c mice are among the most widely used inbred strains in animal experimentation, including investigating visual system abnormalities in autism [2]. Vision in albino mice has long been subject of interest since oculocutaneous albinism in all mammalian species is associated with poor vision [3] due to developmental abnormality in ocular melanin synthesis, resulting in retinal underdevelopment and misrouting of the visual pathway [4]. Few studies have investigated vision capabilities in albino mice, however with some inconsistency. Some studies using virtual-reality optomotor head-tracking response/ reflex (OMR) in BALB/c mice were unable to elicit a measurable response [5, 6], while in another study in BALB/c mice [7], investigators were able to measure a small OMR in the direction opposite to that of the visual stimulus, resulting in a visual acuity (0.12 cyc/deg) lower than that reported for pigmented C57BL/6 mice (B6) (0.5–0.6 cyc/deg) [8]. BALB/c mice, in contrast to other common inbred strains, are reported to be unable to learn a two-alternative swim task (VWT) to evaluate visual acuity [9], while another study used the VWT to assess the visual acuity (0.3 cyc/deg) of BALB/c mice [7].

The pattern electroretinogram (PERG) [10] and pattern visual evoked potentials (PVEPs) have been extensively used to measure acuity and contrast thresholds in both wild-type and mutant mice [11–13]. In the present study we have used PERG and PVEP to assess visual acuity at retinal and cortical level in BALB/c and B6 mice and have also compared PERG/PVEP results with corresponding assessments obtained with OMR.

Methods

Visual acuity assessment by Pattern Electroretinogram (PERG)

The study was performed in B6 mice (4 months old, n = 10, 20 eyes) and BALB/c mice (4 months old, n = 10, 20 eyes) purchased from Jackson Labs (Bar Harbor, ME, USA). All procedures were performed in compliance with the Association for Research in Vision and Ophthalmology (ARVO) statement for use of animals in ophthalmic and vision research. The experimental protocol was approved by the Animal Care and Use Committee of the University of Miami (Project protocol number: 16–247). All mice were maintained in a cyclic light environment (12 h light: 50 lux–12 h: dark) and fed with a grain-based diet (Lab Diet, 500, Opti-diet; PMI Nutrition International, Inc., Brentwood, MO, USA). The PERG was recorded simultaneously from each eye using one common subcutaneous stainless steel needle in the snout as previously described [14]. In brief, mice were anesthetized by means of intraperitoneal injections (0.01 mL/g) of a anesthesia mixture. The mixture contains 1.5 mL ketamine (100 mg/mL), 1.5 mL xylazine (20 mg/mL), and 7 mL injectable sterile water. Mice were gently restrained using a mouth bite bar and a nose holder that allows unobstructed vision and kept at a constant body temperature of 37.0˚C using a feedback-controlled heating pad. Under these conditions the eyes of mice are naturally wide open and in a stable position, with pupils pointing laterally and upward. Visual stimuli were black-white horizontal gratings of 100% contrast and of different spatial frequencies (0.047–0.571 cyc/deg) generated on two (15 cm x 15 cm) LED displays (mean luminance 700 candela/m^2 (cd/m^2) for visual acuity testing at high luminance or 70 cd/m^2 for visual acuity testing at low luminance, and presented to each eye independently (Jorvec Corp, Miami, FL, USA). Pattern stimuli reversed at slight different rates for each eye (OD, 1.016 Hz; OS, 1.008 Hz) to allow mathematical deconvolution of the response and isolation of independent monocular PERG waveforms using one channel continuous acquisition and phase-locking average (OD: 372 sequential epochs of 492 ms each; OS: 372 sequential epochs of 496 ms each) [14]. Due to necessity to record responses to multiple spatial frequencies within the limited timeframe of anesthesia duration, we adopted a fast-recording protocol with limited averaging instead of standard robust averaging [14]. This resulted in a relatively large variability of PERG and noise amplitudes, which did not preclude estimation of acuity as variability across spatial frequency was accounted for by interpolation of amplitude data with linear regressions to the median noise amplitude. Noise waveforms were obtained by averaging odd and even epochs in counterphase. For each spatial frequency, the PERG and noise amplitudes were automatically measured from peak to trough in the time window 50–350 ms. The spatial frequency at which the linear regression of PERG amplitude vs. spatial frequency intercepted the median noise level was considered as the PERG spatial resolution (PERG acuity). For each mouse, the complete recording sequence (lowest to highest spatial frequency) required about 40 minutes, which approximately coincided with the duration of anesthesia. We used a low-to-high spatial frequency recording sequence as BALB/c mice were expected to have a low acuity.

Representative examples of PERG waveforms and noise waveforms in B6 and BALB/c at different spatial frequencies are shown in Fig 1A. In order to have an estimate of PERG acuity that was not based on the assumption of linearity between decreasing PERG amplitude and
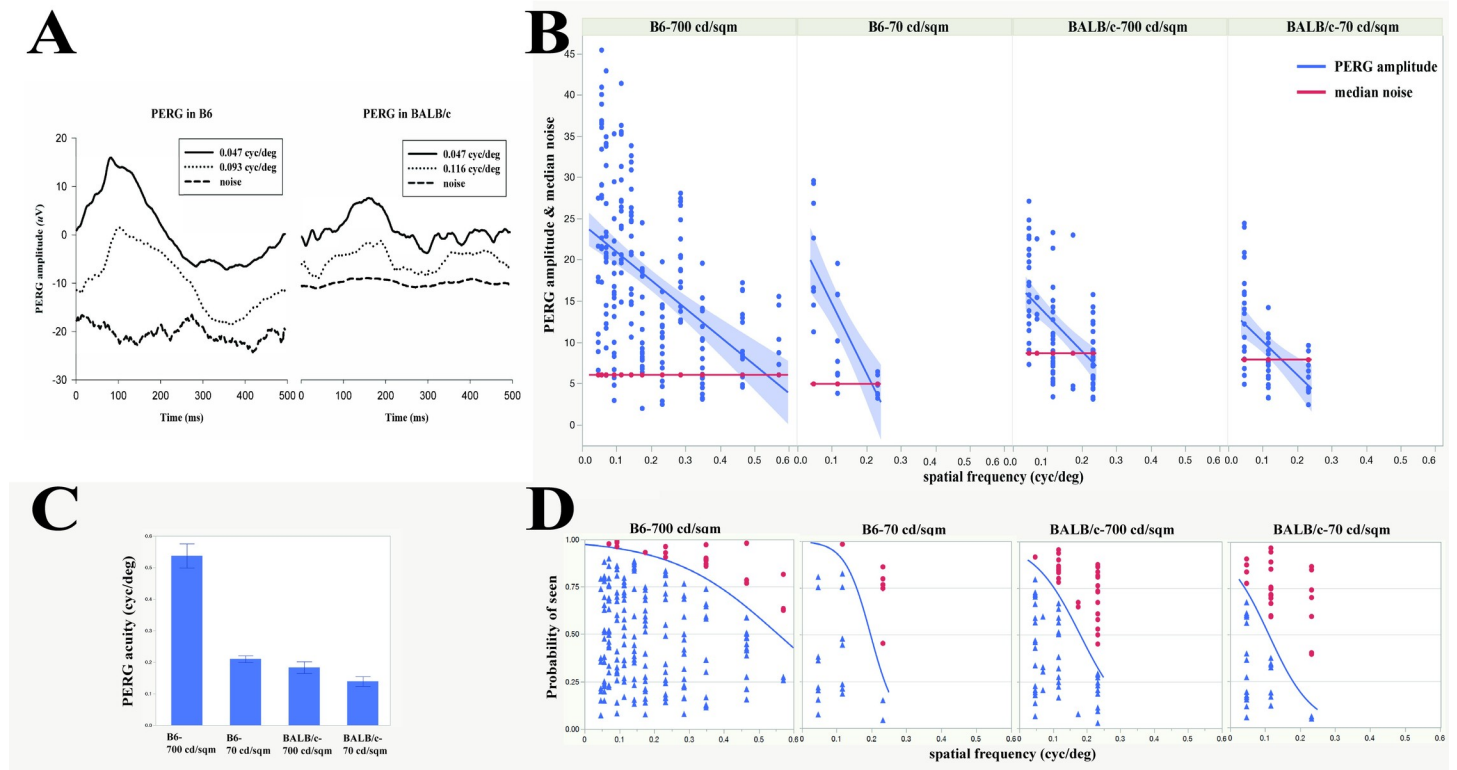
Fig 1. Comparison between PERG acuity of C57BL/6J and BALB/c mice. (A) Examples of PERG and noise waveforms from B6 and BALB/c mice at different spatial frequencies and 700 cd/m² mean luminance. (B) PERG amplitudes as a function of spatial frequency for all mice. Linear regressions of PERG amplitude (blue lines with 95% confidence region) intersect the median noise level (red lines) at different spatial frequencies depending on strain and mean luminance. (C) Mean PERG acuity (± SEM) in B6 and BALB/c in individual mice calculated by linear extrapolation of PERG amplitude to the median noise. (D) Group PERG acuity assessed with the nominal logistic fit showing that acuity depends on strain and luminance. The estimated acuity is the intersection of the logistic curve (blue line) with the 0.50 probability grid line). Data points (blue triangles: SNRs >1, YES; red circles: SNRs ≤1, NO) are jittered along the vertical axis, with no reference to the axis probability scale.

increasing spatial frequency, we calculated for each SF the signal-to-noise ratio (SNR). SNRs > 1 were assigned a categorical value of YES while SNRs ≤ 1 were assigned the value of NO. Data were then submitted to a logistic regression analysis to retrieve the spatial frequency at which YES responses had 50% probability.

Visual acuity assessment by Pattern Visual Evoked Potential (PVEP)

The study was performed in a subset of B6 mice (4 months old, n = 5, 10 eyes) and BALB/c mice (4 months old, n = 5, 10 eyes) purchased from Jackson Labs (Bar Harbor, ME, USA). PVEPs were recorded in anesthetized mice as described in PERG methods section, with the difference that recording electrodes were stainless steel screws (shaft length 2.4 mm, shaft diameter 1.57 mm; PlasticsOne, Roanoke, VA, USA) inserted into the skull, contralateral to the stimulated eye 2 mm lateral to the lambda suture, which corresponds to the monocular visual cortex [11]. Reference electrodes were also stainless steel screws inserted into the skull ipsilateral to the stimulated eye 2 mm lateral to the lambda suture. The ground electrodes were subcutaneous stainless steel needles at the base of the tail. PVEP signals were amplified (10,000 fold) band pass filtered (1–100 Hz) and averaged (two consecutive, partial averages of 600 epochs each, whose grand-average constituted the PVEP response) [15]. For each spatial frequency, PVEP and noise amplitudes were measured from peak to trough. PVEP amplitudes for all mice were plotted as a function of spatial frequency and data interpolated with a linear
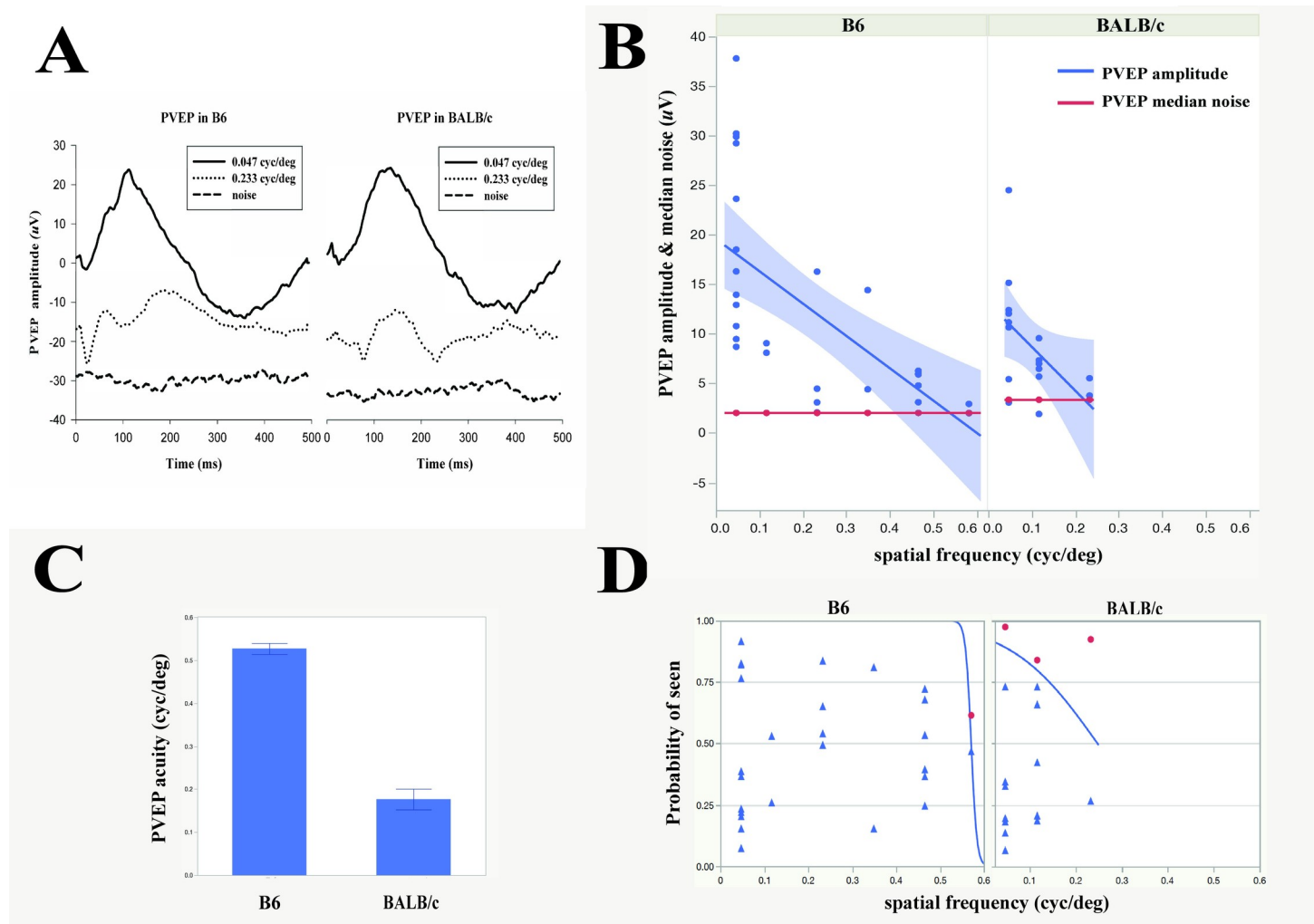
Fig 2. Comparison between PVEP acuity of C57BL/6J and BALB/c mice. (A) Examples of PVEP and noise waveforms recorded from B6 and BALB/c mice at different spatial frequencies and 700 cd/m² mean luminance. (B) PVEP amplitudes as a function of spatial frequency for all mice. Linear regressions of PVEP amplitude (blue lines with 95% confidence region) intersect the median noise level (red lines) at different spatial frequencies depending on strain. (C) Mean PVEP acuity (± SEM) in B6 and BALB/c calculated by linear extrapolation of PVEP amplitude to the median noise in individual mice. (D) Group PVEP acuity assessed with the nominal logistic fit method. The estimated acuity is the intersection of the logistic curve (blue line) with the 0.50 probability grid line). Data points (blue triangles: SNRs >1, YES; red circles: SNRs ≤1, NO) are jittered along the vertical axis, with no reference to the axis probability scale.

regression. The spatial frequency at which the linear regression of PVEP amplitude intercepted the median noise level was considered the PVEP spatial resolution (PVEP acuity). A representative example of PVEP waveforms and noise waveforms at different spatial frequencies is shown in Fig 2A. As for the PERG, PVEP acuities were also calculated using logistic regression of categorical variables (SNR >1: YES; SNR ≤ 1: NO) as a function of spatial frequency. PVEP acuity was considered 50% probability of YES responses.

Visual acuity assessment by optomotor head-tracking response/ reflex (OMR)

Visual acuity was also assessed in B6 and BALB/c mice (n = 5 for each strain) using the optomotor reflex-based spatial frequency threshold test [8, 16, 17]. In brief, mice were placed on a raised platform at the center of a square box surrounded by four LCD monitors displaying

vertical white and black square-wave gratings in horizontal motion (12 degree/second, clockwise/ counterclockwise direction). A customized program controlled the direction of motion and the stimulus spatial frequency in six steps (0.0275, 0.055, 0.11, 0.22, 0.44 and 0.88 cyc/deg). A camera placed above the mouse monitored head movements, which were viewed on a display by an observer unaware of the direction of the stimulus who scored head-tracking reflex (with head-tracking reflex "1"; without head-tracking reflex "0"). OMRs were assessed over at least five trials for each spatial frequency and scored in a blind fashion based on whether the mice tracked the direction of stripe movement with their head. If OMRs tended to be random, then the stimulus spatial frequency was increased stepwise by a factor of 2 until the mouse was unresponsive. All OMR scores were submitted to a categorical (YES: present OMR; NO: absent OMR) logistic regression analysis to determine visual acuity as the highest spatial frequency yielding a 50% probability of present OMR.

Statistics

All analyses were conducted using JMP Pro 14.2 software (SAS Institute Inc., Cary, NC, USA). PERG and PVEP of amplitudes as a function of spatial frequency were fitted with linear regression, whose intercepts with the median noise level were considered as the corresponding spatial resolution (acuity). PERG and PVEP amplitudes were also expressed as categorical variables for presence or absence of response (SNR >1: YES; SNR $\leq$ 1: NO) and data submitted to a logistic regression to determine acuity as the highest spatial frequency with at least 50% probability of YES responses. A similar logistic regression was also used to analyze categorical OMR responses.

Results

PERG acuity

Examples of PERG waveforms recorded in B6 and BALB/c mice at different spatial frequencies are shown in Fig 1A. Fig 1B shows that in both B6 and BALB/c mice, the PERG amplitude at 0.025–0.05 cyc/deg was on average considerably larger than the median noise level, and then progressively decreased with increasing spatial frequency. As the useful time window for recording the entire spatial frequency series was limited by anesthesia duration, we choose a fast-recording protocol with limited averaging that resulted in a relatively high variability of PERG and noise amplitudes compared to standard methods with robust averaging at a single spatial frequency. PERG variability was accounted for in the linear regression of all amplitude data. Noise variability across spatial frequency was accounted for by the use of the median noise. For each strain and condition, a linear regression interpolating all amplitude data intersected the median noise amplitude at a given spatial frequency (PERG acuity). PERG acuities depended on strain and stimulus mean luminance. Extrapolated PERG acuities were: 0.53 cyc/deg (B6-700 cd/ m^2) and 0.22 cyc/deg (B6-70 cd/m^2) and 0.19 cyc/deg (BALB/c-700 cd/ m^2) and 0.15 cyc/deg (BALB/c-70 cd/m^2).

PERG acuities were calculated with the same linear regression approach in individual mice (Fig 1C) The average PERG acuities were, B6-700 cd/ m^2: 0.54 cyc/deg; B6-70 cd/ m^2: 0.21 cyc/deg; BALB/c-700 cd/ m^2: 0.18 cyc/deg; BALB/c-70 cd/ m^2: 0.14 cyc/deg. Statistical analysis showed a strong effect of spatial frequency (p<0.0001), strain (p<0.0001) and luminance (p = 0.0007). The median noise level was higher in BALB/c that in B6 mice at both high and low luminance (Kruskal-Wallis, p<0.001, post-hoc Wilcoxon, p<0.01). To have an alternative acuity estimate, signal-to-noise ratios (PERG amplitude / Noise amplitude) were also calculated and converted to categorical variables (SNR >1: response; SNR $\leq$ 1: no response). Logistic categorical regression was used to predict the highest spatial frequency with at least 50%

probability of responses with SNR>1 (Fig 1D). Logistic regression showed a strong effect of spatial frequency and strain (p<0.001) and a borderline effect of luminance (p = 0.05). PERG acuities evaluated with the logistic regression method were, B6-700 cd/ m^2: 0.54 cyc/deg (p<0.0001); B6-70 cd/ m^2: 0.28 cyc/deg (p = 0.0006); BALB/c-700 cd/ m^2: 0.12 cyc/deg (p<0.0001); BALB/c-70 cd/ m^2: 0.06 cyc/deg (p = 0.0009).

PVEP acuity

Examples of PVEP and noise waveforms obtained from B6 and BALB/c mice with LED display luminance of 700 cd/m^2 are shown in Fig 2A. We used three different analytical approaches to estimate PVEP acuities in B6 and BALB/c. Linear regressions of PVEP amplitudes to corresponding median noises yielded group PVEP acuities of 0.55 cyc/deg in B6 and 0.2 cyc/deg in BALB/c mice (Fig 2B), which were similar to mean acuities calculated from individual mice (0.53 cyc/deg in B6 and 0.18 cyc/deg in BALB/c) (Fig 2C). PVEP acuity estimated from logistic regression of categorical (SNRs >1: Yes; ≤1: No) (Fig 2D) yielded comparable acuities of 0.55 cyc/deg in B6 (p = 0.015) and 0.22 cyc/deg in BALB/c (p = 0.28).

OMR acuity

Fig 3 summarizes OMR results. B6 mice exhibited a clear head-tracking movement with the direction of the rotating pattern stimulus as expected, resulting in OMR visual acuity of 0.44
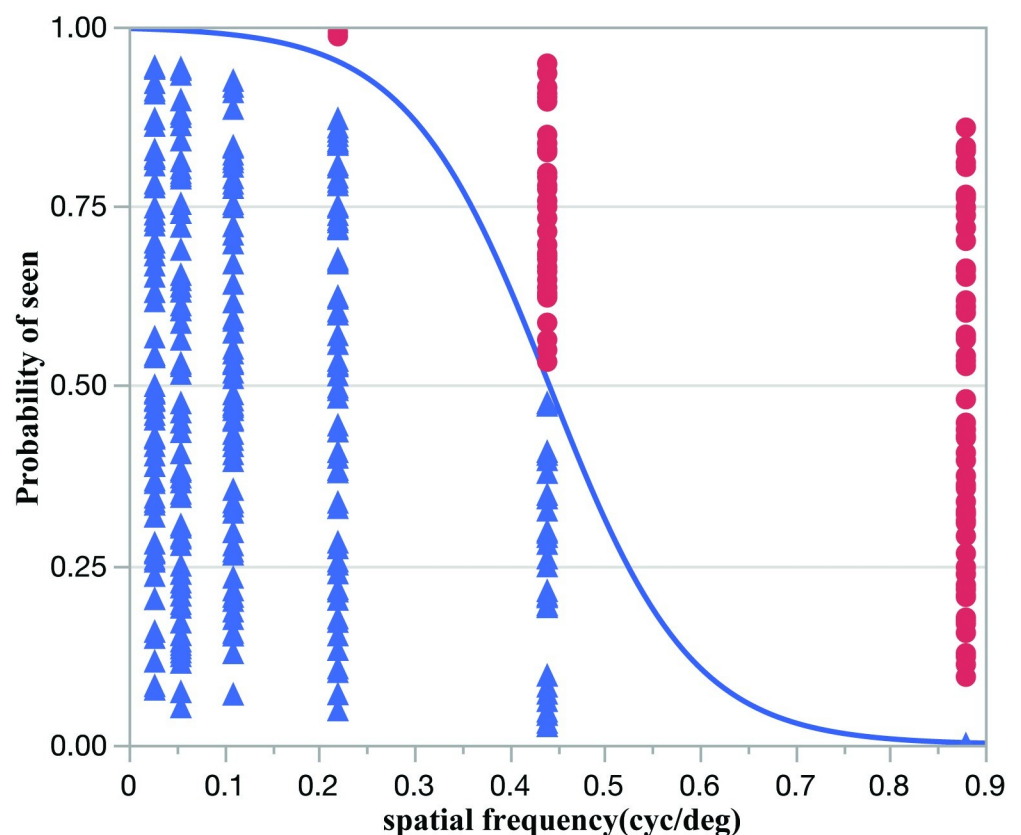

Fig 3. OMR acuity assessed with the nominal logistic fit in C57BL/6J mice. The estimated acuity is the intersection of the logistic curve (blue line) with the 0.50 probability grid line. Data points (blue triangles: SNRs >1, YES; red circles: SNRs ≤1, NO) are jittered along the vertical axis, with no reference to the axis probability scale. Nominal logistic fit of BALB/c mice is not shown as they were unresponsive to the OMR stimulus.

cyc/deg using the categorical logistic approach. Logistic regression showed a strong effect of spatial frequency (p<0.0001). BALB/c mice were virtually unresponsive at any spatial frequency. Weak head-tracking responses were occasionally detected but they were random and could not be used to assess visual acuity.

Discussion

Despite the widespread use of inbred albino mice in research involving the visual pathway, few studies have dealt with the actual assessment of visual performance in this strain [5, 7]. Available studies concur that the visual acuity of BALB/c mice is lower than that of pigmented B6 mice, but do not clarify whether the reduced acuity is due to retinal and/or postretinal abnormalities. The present study used combined recording of PERG and PVEP to have an objective assessment of spatial resolution (acuity) at retinal and cortical level. The PERG signal of BALB/c mice, as that of B6 mice, reflects RGC activity as the response is abolished after lesion of the optic nerve that causes RGC degeneration while leaving pre-ganglionic retinal neurons intact [18, 19]. Thus, PERG acuity reflects the spatial resolution of the retinal output. To minimize bias in spatial resolution assessment, we used both linear and logistic regression of PERG/PVEP amplitude data as well as OMR behavior. Despite substantial variability of raw data, different methods yielded consistent estimates of spatial resolution. Namely, our results showed that the mean PERG acuity of BALB/c mice was 0.16 cyc/deg and that of B6 mice was 0.54 cyc/deg, calculated with either linear regression of PERG amplitude or logistic regression of categorical SNR>1. By decreasing the stimulus mean luminance from 700 cd/m^2 to 70 cd/m^2, mean PERG acuity decreased significantly by half in B6 and decreased insignificantly (p = 0.76) in BALB/c mice (Fig 1D). Psychophysical visual acuity reduction with decreasing luminance is a well-known phenomenon in pigmented mammals [20–24]. However, visual acuities in albinism do not appear to have an obvious luminance-acuity relationship at it has been reported to occur in albinism [25, 26].

In both B6 and BALB/c mice, PERG acuity matched PVEP acuity, suggesting that in both strains the visual acuity was primarily determined at retinal level with no further change along the post-retinal visual pathway. Selective loss of spatial resolution in the post-retinal pathway may occur in mutant B6 mice lacking the β2 subunit of the neuronal nicotinic receptor, where PERG acuity is reported to be 0.6 cyc/deg compared to PVEP acuity of 0.3 cyc/deg [12]. In B6 mice, we were able to compare PERG acuity with OMR acuity and found that they were similar. We were unable to elicit a measurable OMR reflex in BALB/c mice, in agreement with other studies [5]. We cannot exclude that a more sophisticated OMR method could have detected small OMR reflexes that allowed assessment of visual acuity [8].

The causes of reduced retinal acuity in BALB/c mice may be associated to the reported reduction of rod density [4, 27], retinal thickness [7, 28], and flash-ERG response [29] that reflects outer retinal activity. Other mechanisms may contribute, as the PERG is a cone-driven response that depends on RGC density as well as intraretinal connectivity [30, 31]. The present results showed that PERG amplitude was reduced in BALB/c mice while the noise was increased. Both reduced amplitude and increased noise contributed to reduction of retinal acuity. Reported defects of the post-retinal pathway [7, 32] did not cause incremental reduction of PVEP acuity but impaired the OMR.

Conclusions

The present results show that electrophysiological acuity determined with non-invasive, high-throughput methods that test two eyes simultaneously can be assessed in both B6 mice and BALB/c mice. This may be advantageous compared to either operant methods that require

training and learning and may not be feasible in some strains or OMR method at which BALB/c mice may be poorly responsive. Also, PERG/PVEP methods may be advantageous compared to both operant and OMR methods as these do not identify the locus of visual defect along the visual pathway.

Supporting information

S1 Dataset.
(XLSX)

Author Contributions

Conceptualization: Vittorio Porciatti, Tsung-Han Chou.

Data curation: Michelle Braha, Vittorio Porciatti, Tsung-Han Chou.

Formal analysis: Vittorio Porciatti, Tsung-Han Chou.

Funding acquisition: Vittorio Porciatti.

Investigation: Vittorio Porciatti, Tsung-Han Chou.

Methodology: Michelle Braha, Vittorio Porciatti, Tsung-Han Chou.

Project administration: Vittorio Porciatti.

Resources: Vittorio Porciatti.

Supervision: Vittorio Porciatti, Tsung-Han Chou.

Validation: Michelle Braha, Vittorio Porciatti, Tsung-Han Chou.

Visualization: Michelle Braha, Vittorio Porciatti, Tsung-Han Chou.

Writing – original draft: Tsung-Han Chou.

Writing – review & editing: Michelle Braha, Vittorio Porciatti, Tsung-Han Chou.

References

1. Leinonen H, Tanila H. Vision in laboratory rodents-Tools to measure it and implications for behavioral research. Behav Brain Res. 2018; 352:172–82. https://doi.org/10.1016/j.bbr.2017.07.040 PMID: 28760697

2. Traber GL, Chen CC, Huang YY, Spoor M, Roos J, Frens MA, et al. Albino mice as an animal model for infantile nystagmus syndrome. Invest Ophthalmol Vis Sci. 2012; 53(9):5737–47. https://doi.org/10.1167/iovs.12-10137 PMID: 22789924

3. Creel DJ. Visual and Auditory Anomalies Associated with Albinism. In: Kolb H, Fernandez E, Nelson R, editors. Webvision: The Organization of the Retina and Visual System. Salt Lake City (UT)1995.

4. Jeffery G, Brem G, Montoliu L. Correction of retinal abnormalities found in albinism by introduction of a functional tyrosinase gene in transgenic mice and rabbits. Brain Res Dev Brain Res. 1997; 99(1):95–102. https://doi.org/10.1016/s0165-3806(96)00211-8 PMID: 9088570

5. Puk O, Dalke C, Hrabe de Angelis M, Graw J. Variation of the response to the optokinetic drum among various strains of mice. Front Biosci. 2008; 13:6269–75. https://doi.org/10.2741/3153 PMID: 18508659

6. Barabas P, Huang W, Chen H, Koehler CL, Howell G, John SW, et al. Missing optomotor head-turning reflex in the DBA/2J mouse. Invest Ophthalmol Vis Sci. 2011; 52(9):6766–73. https://doi.org/10.1167/iovs.10-7147 PMID: 21757588

7. Yeritsyan N, Lehmann K, Puk O, Graw J, Lowel S. Visual capabilities and cortical maps in BALB/c mice. Eur J Neurosci. 2012; 36(6):2801–11. https://doi.org/10.1111/j.1460-9568.2012.08195.x PMID: 22738127

8. Shi C, Yuan X, Chang K, Cho KS, Xie XS, Chen DF, et al. Optimization of Optomotor Response-based Visual Function Assessment in Mice. Sci Rep. 2018; 8(1):9708. https://doi.org/10.1038/s41598-018-27329-w PMID: 29946119

9. Wong AA, Brown RE. Visual detection, pattern discrimination and visual acuity in 14 strains of mice. Genes Brain Behav. 2006; 5(5):389–403. https://doi.org/10.1111/j.1601-183X.2005.00173.x PMID: 16879633

10. Porciatti V, Pizzorusso T, Cenni MC, Maffei L. The visual response of retinal ganglion cells is not altered by optic nerve transection in transgenic mice overexpressing Bcl-2. Proc Natl Acad Sci U S A. 1996; 93 (25):14955–9. https://doi.org/10.1073/pnas.93.25.14955 PMID: 8962163

11. Porciatti V, Pizzorusso T, Maffei L. The visual physiology of the wild type mouse determined with pattern VEPs. Vision Res. 1999; 39(18):3071–81. https://doi.org/10.1016/s0042-6989(99)00022-x PMID: 10664805

12. Rossi FM, Pizzorusso T, Porciatti V, Marubio LM, Maffei L, Changeux JP. Requirement of the nicotinic acetylcholine receptor beta 2 subunit for the anatomical and functional development of the visual system. Proc Natl Acad Sci U S A. 2001; 98(11):6453–8. https://doi.org/10.1073/pnas.101120998 PMID: 11344259

13. Gianfranceschi L, Siciliano R, Walls J, Morales B, Kirkwood A, Huang ZJ, et al. Visual cortex is rescued from the effects of dark rearing by overexpression of BDNF. Proc Natl Acad Sci U S A. 2003; 100 (21):12486–91. https://doi.org/10.1073/pnas.1934836100 PMID: 14514885

14. Chou TH, Toft-Nielsen J, Porciatti V. High-Throughput Binocular Pattern Electroretinograms in the Mouse. Methods Mol Biol. 2018; 1695:63–8. https://doi.org/10.1007/978-1-4939-7407-8_6 PMID: 29190018

15. Chou TH, Tomarev S, Porciatti V. Transgenic mice expressing mutated Tyr437His human myocilin develop progressive loss of retinal ganglion cell electrical responsiveness and axonopathy with normal iop. Invest Ophthalmol Vis Sci. 2014; 55(9):5602–9. https://doi.org/10.1167/iovs.14-14793 PMID: 25125600

16. Prusky GT, Alam NM, Beekman S, Douglas RM. Rapid quantification of adult and developing mouse spatial vision using a virtual optomotor system. Invest Ophthalmol Vis Sci. 2004; 45(12):4611–6. https://doi.org/10.1167/iovs.04-0541 PMID: 15557474

17. Kretschmer F, Kretschmer V, Kunze VP, Kretzberg J. OMR-arena: automated measurement and stimulation system to determine mouse visual thresholds based on optomotor responses. PLoS One. 2013; 8 (11):e78058. https://doi.org/10.1371/journal.pone.0078058 PMID: 24260105

18. Xia X, Wen R, Chou TH, Li Y, Wang Z, Porciatti V. Protection of pattern electroretinogram and retinal ganglion cells by oncostatin M after optic nerve injury. PLoS One. 2014; 9(9):e108524. https://doi.org/10.1371/journal.pone.0108524 PMID: 25243471

19. Liu Y, McDowell CM, Zhang Z, Tebow HE, Wordinger RJ, Clark AF. Monitoring retinal morphologic and functional changes in mice following optic nerve crush. Invest Ophthalmol Vis Sci. 2014; 55(6):3766–74. https://doi.org/10.1167/iovs.14-13895 PMID: 24854856

20. Cavonius CR, Robbins DO. Relationships between luminance and visual acuity in the rhesus monkey. J Physiol. 1973; 232(2):239–46. https://doi.org/10.1113/jphysiol.1973.sp010267 PMID: 4199366

21. Abdeljalil J, Hamid M, Abdel-Mouttalib O, Stephane R, Raymond R, Johan A, et al. The optomotor response: a robust first-line visual screening method for mice. Vision Res. 2005; 45(11):1439–46. https://doi.org/10.1016/j.visres.2004.12.015 PMID: 15743613

22. Hayes JM, Balkema GW. Visual thresholds in mice: comparison of retinal light damage and hypopigmentation. Vis Neurosci. 1993; 10(5):931–8. https://doi.org/10.1017/s0952523800006143 PMID: 8217942

23. Hayes JM, Balkema GW. Elevated dark-adapted thresholds in hypopigmented mice measured with a water maze screening apparatus. Behav Genet. 1993; 23(4):395–403. https://doi.org/10.1007/BF01067442 PMID: 8240220

24. Schmucker C, Seeliger M, Humphries P, Biel M, Schaeffel F. Grating acuity at different luminances in wild-type mice and in mice lacking rod or cone function. Invest Ophthalmol Vis Sci. 2005; 46(1):398–407. https://doi.org/10.1167/iovs.04-0959 PMID: 15623801

25. Summers CG. Vision in albinism. Trans Am Ophthalmol Soc. 1996; 94:1095–155. PMID: 8981720

26. Jacobson SG, Mohindra I, Held R, Dryja TP, Albert DM. Visual acuity development in tyrosinase negative oculocutaneous albinism. Doc Ophthalmol. 1984; 56(4):337–44. https://doi.org/10.1007/BF00155678 PMID: 6425027

27. Donatien P, Jeffery G. Correlation between rod photoreceptor numbers and levels of ocular pigmentation. Invest Ophthalmol Vis Sci. 2002; 43(4):1198–203. PMID: 11923266

28. Zhang P, Goswami M, Zawadzki RJ, Pugh EN Jr. The Photosensitivity of Rhodopsin Bleaching and Light-Induced Increases of Fundus Reflectance in Mice Measured In Vivo With Scanning Laser Ophthalmoscopy. Invest Ophthalmol Vis Sci. 2016; 57(8):3650–64. https://doi.org/10.1167/iovs.16-19393 PMID: 27403994

29. Gresh J, Goletz PW, Crouch RK, Rohrer B. Structure-function analysis of rods and cones in juvenile, adult, and aged C57bl/6 and Balb/c mice. Vis Neurosci. 2003; 20(2):211–20. https://doi.org/10.1017/s0952523803202108 PMID: 12916741

30. Sieving PA, Steinberg RH. Proximal retinal contribution to the intraretinal 8-Hz pattern ERG of cat. J Neurophysiol. 1987; 57(1):104–20. https://doi.org/10.1152/jn.1987.57.1.104 PMID: 3559667

31. Saleh M, Nagaraju M, Porciatti V. Longitudinal evaluation of retinal ganglion cell function and IOP in the DBA/2J mouse model of glaucoma. Invest Ophthalmol Vis Sci. 2007; 48(10):4564–72. https://doi.org/10.1167/iovs.07-0483 PMID: 17898279

32. Jeffery G. The albino retina: an abnormality that provides insight into normal retinal development. Trends Neurosci. 1997; 20(4):165–9. https://doi.org/10.1016/s0166-2236(96)10080-1 PMID: 9106357